FEW LAYER GRAPHENES DECORATED WITH SILVER NANOPARTICLES

E. Vermisoglou[1], N. Todorova[1], G. Pilatos[1], G. Romanos[1], V. Likodimos[1], N. Boukos[1], C. Lei[2], F. Markoulidis[2], C. Lekakou[2*], C. Trapalis[1*]

[1] Institute of Advanced Materials, Physicochemical Processes, Nanotechnology and Microelectronics, National Centre for Scientific Research "Demokritos", 153 10, Ag. Paraskevi, Attikis, Greece
[2]Division of Mechanical, Medical, and Aerospace Engineering, Faculty of Engineering and Physical Sciences, University of Surrey, Guildford GU2 7XH, UK

** c.lekakou@surrey.ac.uk , *trapalis@ims.demokritos,gr*

Keywords: graphene, supercapacitors, silver nanoparticles.

Abstract

Graphite oxide (GO) powder was irradiated in a microwave oven and lightweight expanded graphite oxide (EGO) powder with high BET surface area 1316 m^2/g was obtained. Activation of EGO was performed by impregnation in KOH solution and high temperature treatment under Ar flow, followed by annealing in vacuum (t-EGO). KOH acted more as a reducing agent diminishing the defects than as a surface modifier for high porosity. EGO and t-EGO were further decorated with Ag nanoparticles (~40 nm) applying solar light irradiation. Along with Ag deposition the structural defects of the graphene were reduced upon photo-irradiation. It was established that among the bare graphenes the EGO exhibited the highest capacitance. From the Ag-containing composites, the KOH activated EGO acted as a supercapacitor, while the non-activated EGO as a resistant.

1 Introduction

The rise of graphene constitutes an exciting new area in the field of carbon nanoscience triggering thus the academic and technological interest. Graphene's unique mechanical and electronic properties, such as ballistic transport at room temperature combined with chemical and mechanical stability have attracted great attention. These remarkable properties can also extend to bilayer and few-layer graphenes, opening thus a broad field of potential applications [1, 2]. High quality graphene sheets (single layer to a few layers) with superior electrical properties allowed the development of new engineered carbons for energy storage [3]. Recently, they have been used in supercapacitors devices to replace conventional carbon electrodes thus improving their performance. Various methods have been developed to exfoliate graphite and stabilize graphene sheets. These strategies include top down approaches such as: micromechanical cleavage of graphite [2, 4] reduction of graphite oxide, lithography, unzipping of carbon nanotubes [5], and liquid-phase exfoliation [6]. In the present work, we proceed with production of highly exfoliated graphene material according to [7] and activation with KOH which can also act as a reducing agent [8].

It is known that silver decorated Single Wall Carbon Nanotubes (SWCNTs) exhibit higher specific capacitance (106 F g^{-1}) compared to pristine SWCNTs (47 F g^{-1}) utilized in effective bifunctional charge collectors and active electrode materials for supercapacitors [9]. Therefore, Ag-decorated graphene materials are expected to exhibit increased conductivity

and higher specific capacitance since Ag nanoparticles not only accelerate the electron conduction but also improve the proton diffusion throughout the electrode [10]. In the present work, silver nanoparticles were deposited on graphene materials by sunlight irradiation of silver ions which were dispersed initially in these materials.

2 Materials and testing methods

2.1 Samples preparation

Graphite oxide (GO) was synthesized using a modified Staudenmaier's method **[11].** GO was irradiated in a microwave oven (900 W) for 1min and 15sec and a fluffy form of carbon, namely Expanded Graphite Oxide was formed (sample EGO). 0.4 g of this material were added to 20mL aqueous solution KOH (7M, 1.6M), stirred for 4 hours, aged in ambient conditions for 24 hours and dried in oven at 65 ^{o}C. A thermal treatment at 800 ^{o}C for 1hour followed under continuous Ar flow. This material was washed several times until neutral pH. Then annealing at 800 ^{o}C under vacuum was applied for 2 hours and the samples obtained were designated as t-EGO7 and t-EGO1.6. The treatment with KOH 1.6M (loading ~4.5 times the mass of EGO) proved to be more mass efficient than that with KOH 7M (loading ~20 times the mass of EGO) where from ~1g EGO only ~100 mg t-EGO7 were obtained.

EGO and KOH 1.6M activated graphite oxide were further decorated with Ag nanoparticles using solar light irradiation. For this purpose, 0.5 g of each material were mixed with 300 mL distilled water and sonicated for 10 min using Hielscher homogenizer. 2% water solution of $AgNO_3$ (Panreac) was added in weight ratio C:Ag = 2:1. The mixtures were additionally sonicated for 10 min and irradiated for 30 min in solar light simulator (Suntest XLS). After multiple centrifugation-washing the slurries were dried at ambient conditions. The samples obtained were nominated as EGO/Ag and t-EGO1.6/Ag.

2.2 Testing methods

Siemens D500 X-ray diffractometer was used for the XRD measurements. The nitrogen adsorption isotherms at −196 ^{o}C were obtained with the Quantachrome Autosorb-1 MP volumetric apparatus. TEM analysis was carried out in a JEOL 2011 HR-TEM, operating at 200 kV and fitted with an Oxford Instruments INCAx-sight EDS detector. Raman spectra were obtained using an inVia Reflex (Renishaw) micro-Raman spectrometer using objective x 50 with a focal point of 1.5 μm^2 and a laser excitation of 514.5 nm. The IR transmittance spectra of the samples (KBr pellets) were measured on EQUINOX 55/5, Bruker instrument. The prepared materials mixed with 10 wt% carbon black and 5 wt% PVDF, used as binder, were deposited as an electrode layer on aluminium foil used as current collector. Such electrodes were then used to fabricate an electrochemical double layer capacitor (EDLC) cell with 1 M $TEABF_4$/PC electrolyte. The electrochemical properties of the materials were then investigated using impedance spectroscopy in the range 10 mHz-1MHz and cyclic voltammetry (CV) in a voltage range 0-3V.

3 Results and Discussion

When GO is irradiated in a commercial microwave oven an abrupt expansion is taking place resulting in a fluffy material that has a high BET surface area 1316 m^2/g. TEM images (Figure 1) show the layered characteristics of the EGO in a nanometer scale (1a). The second TEM image (1b) is a thickness map that gives by contrast between the thickness of substrate (Cu grid) (dark color) and EGO (light color) a picture of how thin is the layered EGO. TEM images show that the graphene sheets are homogeneous and quite smooth. By comparison of the same graphene area in a bright field TEM image (1a) and the corresponding oxygen map (1c) it can be concluded that after the expansion the remaining oxygen groups of the initial graphite oxide are mainly located at the edges of the graphene sheets and constitute the

defects on EGO material. The existence of individual graphene sheets is evident from the High Resolution TEM image (1d) that also provides information about the number of layers. It is apparent that the microwave expanded graphite oxide consists of a few layers approximately four or less. Conclusively, the violent removal of oxygen functional groups that occurs during the expansion results in exfoliation of graphite oxide to a large extent.

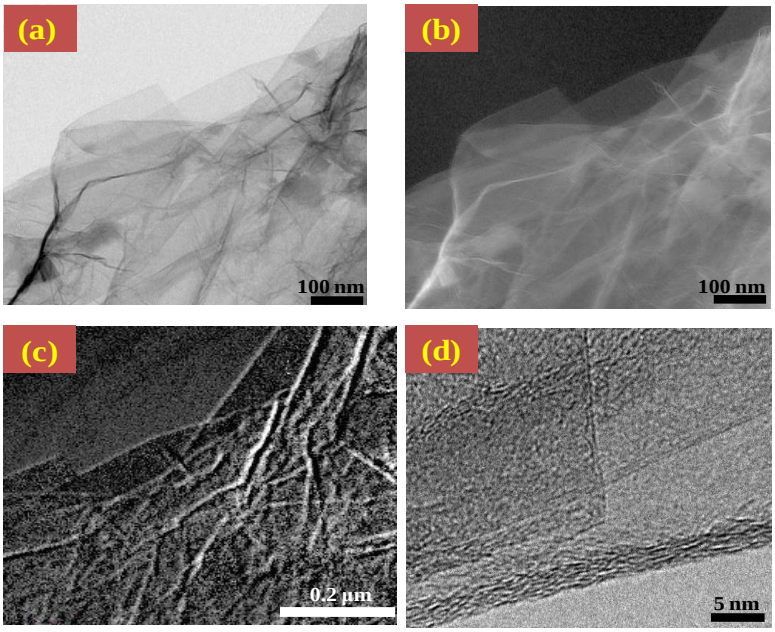

Figure 1. *Bright field TEM image of EGO (a), thickness map (b) and oxygen map (c) of the same graphene area and HRTEM (d) image showing few layer graphenes.*

The above findings were also confirmed by the FTIR results presented in Figure 2. From the IR spectra it is apparent that all the bands related to oxygen functionalities present in the GO were significantly reduced after the expansion of GO through microwave irradiation. The typical peaks of GO appear at 1728 cm^{-1} (C=O carboxyl stretching vibration), 1630 cm^{-1} (C=C in aromatic ring assigned to skeletal vibrations of unoxidized graphite domains and C=O), 1383 cm^{-1} (C–OH stretching) and 1070 cm^{-1} (C–O–C in epoxide).

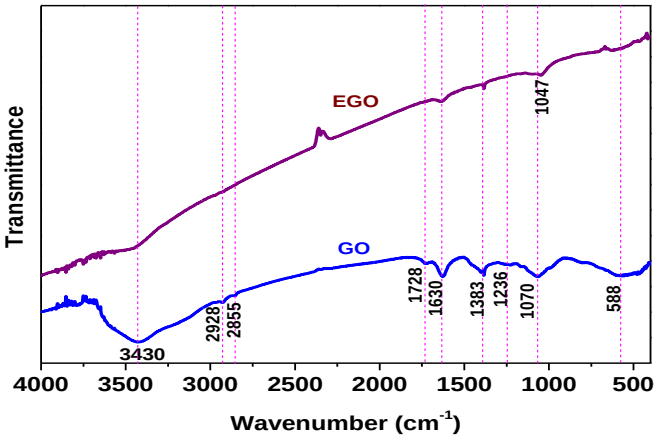

Figure 2. *FTIR spectra of as prepared graphite oxide (GO) and after microwave treatment (EGO).*

The wide peak appearing at 3000–3500 cm^{-1} is related to the presence of hydroxyl groups. The absorption bands at 588 and 803 cm^{-1} are assigned to aromatic C-H bending. These results are in consistence with literature [12, 13]. After the expansion, the bands related to oxygen moieties diminish significantly indicating reduction of GO. The band at ~1047 cm^{-1} in EGO spectrum is attributed to alkoxy groups that were formed after the reduction of carbonyl groups in GO. The band at 3430 cm^{-1} in EGO decays significantly indicating the dehydration of GO. The two peaks at 2928 cm^{-1} and 2855 cm^{-1} resulting from the $–CH_2$ stretching in GO are absent in the case of EGO, while the band at ~1630 cm^{-1} attributed to both C=C and C=O is diminished in the expanded material in comparison to the initial GO. These changes can be attributed to the alleviation of the groups considered as defects in the graphene lattice and re-establishment at least to some extent of the aromatic structure [14].

The structural alteration and the Ag loading of the graphitic materials were investigated by XRD analysis. The obtained patterns of the bare and Ag-decorated graphenes are presented in Figure 3. A well defined peak at 26.5° can be observed for the initial graphite with a basal spacing d_{002} =3.34 Å. In the case of GO a (001) peak appears at 12.0° with a basal spacing of d_{001}= 7.35 Å which is larger compared to that of graphite. This outcome was related to the introduction of oxygenated functional groups on the carbon sheets. After the expansion of GO via microwave irradiation the (001) peak disappeared and a small bump appears at ~26° for EGO and t-EGO1.6. The pattern of t-EGO7 is similar to t-EGO1.6 and for this reason is not presented in the figure. The phenomenon is attributed to the quick removal of many oxygen-containing functional groups, as it was already verified by IR spectra, and further reduction of EGO through thermal treatments that leads to a partial re-stacking of the graphene layers. It must be noted that the peak at ~26° is significantly weaker and broader than that of the pristine graphite. This is an indication that the samples are comprised of free graphene sheets poorly ordered along the stacking direction giving a randomly ordered carbonaceous layered solid with a corrugated structure [13]. For the Ag loaded EGO and t-EGO1.6 materials Ag diffraction signals can be observed (Fig. 3b) that are consistent with JCPDS card Silver-3C syn. # 04-0783. The peaks at 2θ 38.1° and 44.3° are ascribed to the Ag (111) and (200) crystallographic planes, respectively. The average size of the Ag particles in the hybrid materials calculated using Sherrer's equation was found to be 43.5 nm and 40.5 nm for the EGO/Ag and t-EGO1.6/Ag, correspondingly. It must be underlined that the Ag photo-deposition was achieved in water solutions without addition of any sacrificing agent. Also, additional reduction of graphene oxide occurred during photo-irradiation especially for the activated t-EGO1.6 sample. The peak at 2θ=40.6 ° in the pattern of t-EGO1.6/Ag sample was related to this form of graphene oxide [15].

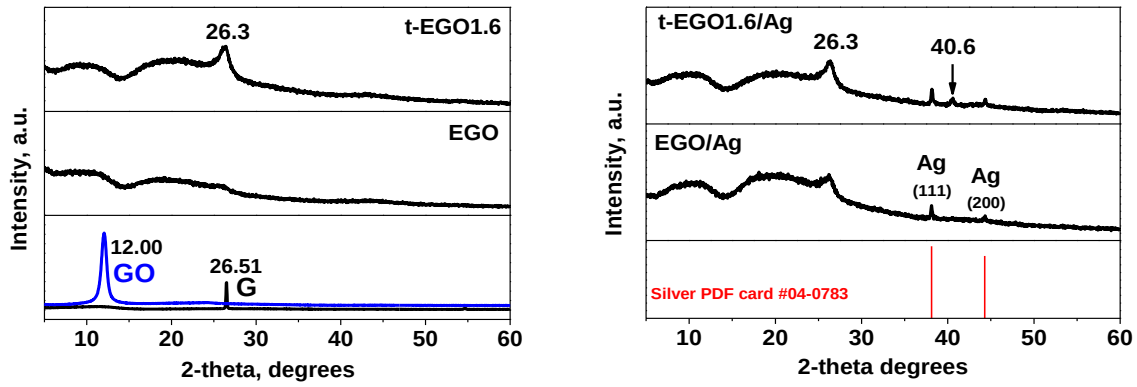

(a) (b)

Figure 3. *XRD pattern of bare (a) and Ag-decorated (b) graphitic materials.*

The activation of EGO with KOH (7M, 1.6M) at high temperature under Ar flow and subsequent thermal annealing resulted in t-EGO7 and t-EGO1.6 with BET surface area 216 m^2/g and 186 m^2/g, accordingly.

The impact of thermal treatments and decoration with Ag nanoparticles is outlined in Raman spectra (Figure 4). The G and D bands are associated with the ordered sp^2 carbon and disordered defects and edge carbons, respectively. The wavenumber positions (1586 cm^{-1}, 1356 cm^{-1}) and relative peak intensities of the G and D bands I_D/I_G=0.13 (t-EGO7) in comparison with I_D/I_G =0.71 for EGO indicate that the carbon in the annealed sample is nearly all sp^2 in hybridization, emphasizing the high quality of the crystal lattice in t-EGO7 sample. In fact, the decrease of D band's intensity is attributed to graphite ''self-healing'' by heat reduction [16]. The small D band (1356 cm^{-1}) may be edge-related, where the edges of the flakes and also the borderline between sections of different heights contribute to the D band signal, while the inner parts of the flakes do not [17]. Interestingly, the I_D/I_G= 0.13 of t-EGO7 is much lower than most chemical reduction reports, such as $NaBH_4$ (>1), hydrothermal reduction (0.90), hydrazine hydrate (1.63), implying that the combination of activation with KOH (800 ^oC) and the thermal annealing route is more effective than other reduction processes **[**18]. The I_D/I_G peak intensity ratio, the shape and full width at half maximum (FWHM) of the 2D peak have been used to characterize few-layer graphene. The 2D peak has a symmetric shape with FWHM ~58 cm^{-1}corresponding to ~4 layers [19]. These results and the TEM study, indicate the presence of few layer graphene.

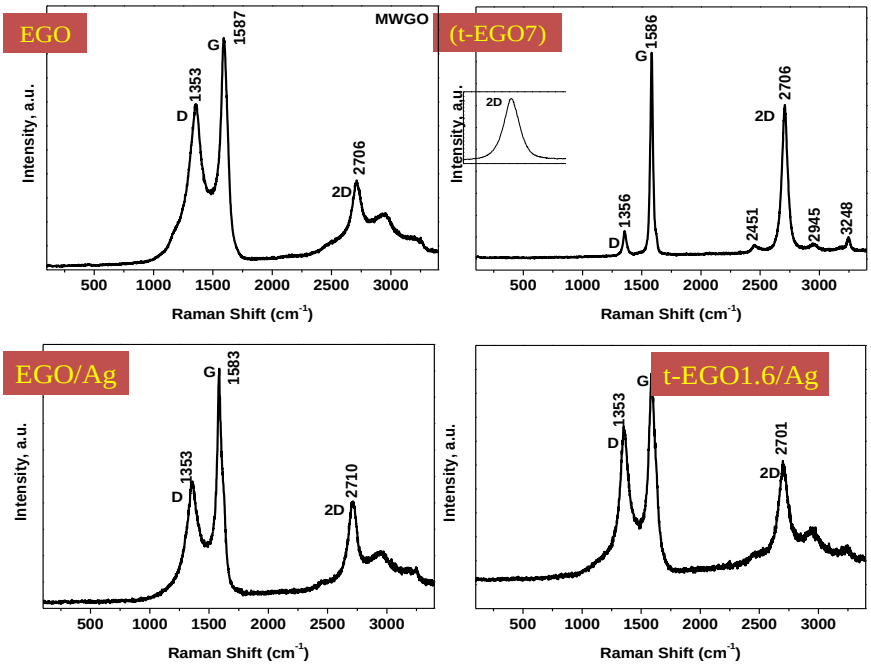

Figure 4. *Raman spectra of: microwave expanded graphite oxide (EGO); EGO after activation with KOH (t-EGO7) inset: a segment of 2D peak of t-EGO7); Ag- decorated EGO and t-EGO1.6 materials (EGO/Ag and t-EGO1.6/Ag respectively).*

The role of KOH in order to improve porosity has been already explained in literature [7] where it is suggested that the activation of carbon with KOH proceeds through the formation of K_2CO_3 and its consequent decomposition. However, KOH is also known as a reduction agent assisting a green route for the reduction of GO. Exfoliated GO undergoes quick deoxygenation in strong alkali solutions even at moderate temperatures [8] which in our experiment (800 ^oC) was more facilitated. In addition, due to evaporation but not filtration of the EGO-KOH mixture the loading of EGO with KOH was approximately 20 and 4.5 times

its weight for the samples t-EGO7 and t-EGO1.6, respectively. Subsequently, instead of creating a network of micropores KOH reacted with the material, resulting in removing domains of it and significant mass loss.

The recorded Raman signals of the hybrid materials EGO/Ag and t-EGO1.6/Ag were enhanced in comparison to the bare samples. The outcome was related to the surface-enhanced Raman scattering (SERS) activity owing to the charge transfer interaction of EGO with Ag nanoparticles [20]. For the sample EGO/Ag the I_D/I_G ratio is lower than in corresponding non-doped material indicating less defects and higher quality of the composite materials. In sample t-EGO1.6/Ag the 2D peak in Raman spectrum is symmetric and more intense than in EGO that can be attributed to both KOH treatment and solar light irradiation in the presence of Ag.

The Nyquist plots of the capacitor cells with graphene and graphene/Ag composite materials as well as their capacitance performance are presented in Figure 5. From the Nyquist plots (Fig. 5 a, b) it can be observed that EGO has the lowest in-series resistance, lowest transfer resistance, and highest capacitance. This outcome was accredited to the highest BET specific surface area of the sample (1316 m^2/g).

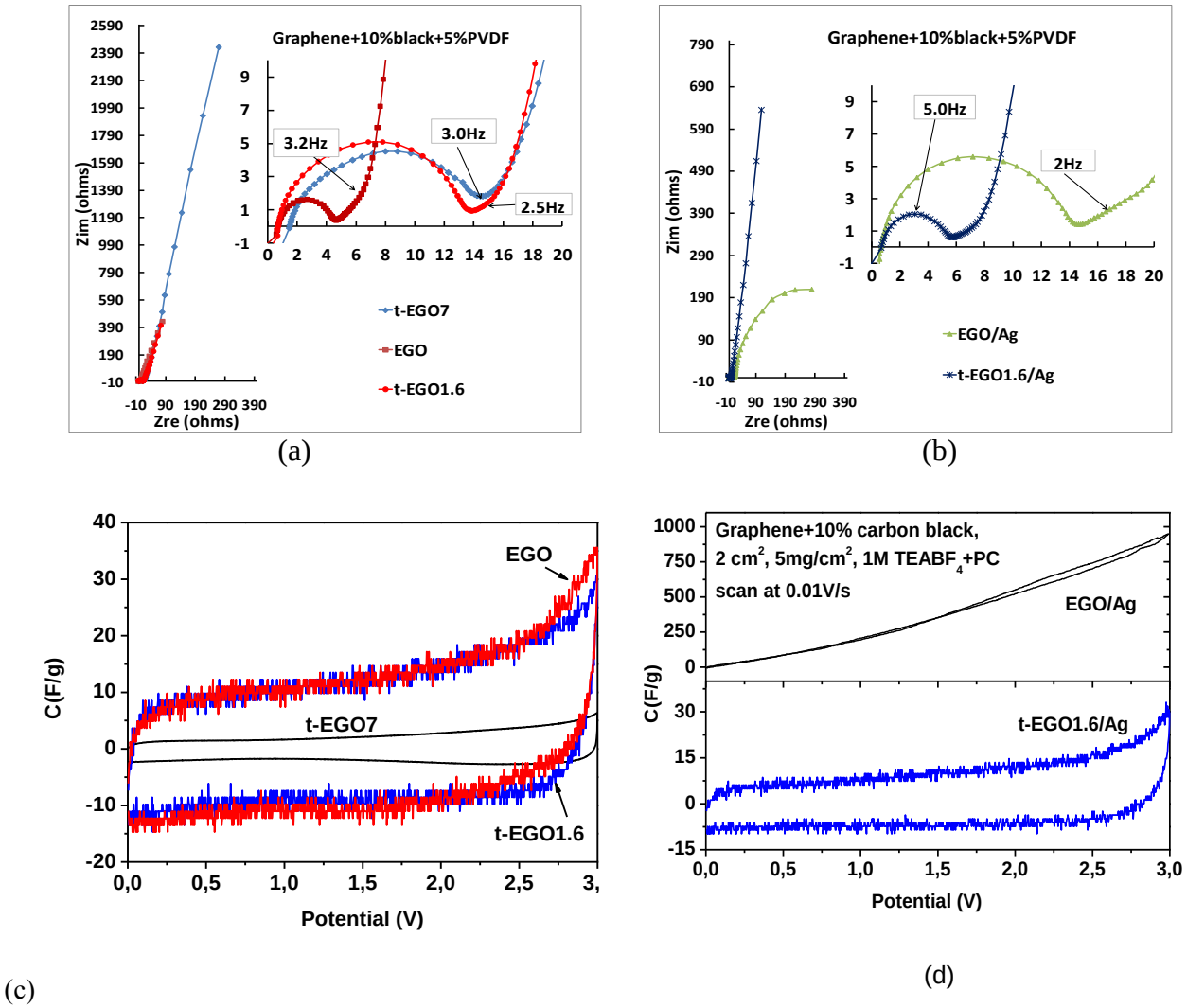

Figure 5. *Impedance plots of capacitor cells with bare (a) and Ag-decorated (b) graphene samples; specific capacitance of bare (c) and Ag-decorated (d) materials.*

The KOH activated sample t-EGO1.6 has also high capacitance. In t-EGO1.6/Ag the deposition of Ag increases the conductivity but also decreases the capacitance to some extent, possibly due to the fact that the Ag nanoparticles fill the pores of t-EGO1.6 and decrease it's BET without large amount of pillaring between graphene sheets. The cell with EGO/Ag does not display supercapacitor behaviour. The capacitance performance of the materials is further illustrated in the CV plots (Fig. 5 c, d) for all electrode materials. The CV plots show that EGO/Ag–based cell is purely a resistor possibly due to low effective porosity.

4 Conclusions

Production of few layer graphenes and their decoration with Ag nanoparticles was achieved through microwave expansion of graphite oxide, KOH activation and subsequent photo-deposition of Ag nanoparticles in water without addition of sacrificial agent.

Reduction of graphite oxide occurred during microwave treatment resulting in lightweight EGO material with high specific surface area showing the highest capacitance ofm the materials investigated.

The activation with KOH diminished significantly the defects especially in high concentrations. However, it was accompanied with decrease of capacitance, significant loss of mass and partial re-stacking.

Along with Ag deposition the structural defects of the graphene, namely I_D/I_G ratio, were reduced upon photo-irradiation. The KOH activated EGO with Ag nanoparticles acted as a supercapacitor, while the non-activated EGO with Ag did not display supercapacitor behavior.

References

[1] Geim A. K., Novoselov K. S. The rise of graphene. *Nature Materials*, **6**, 183-191 (2007).

[2] Ferrari A.C., Meyer J.C., Scardaci V., Casiraghi C., Lazzeri M., Mauri F., Piscanec S., Jiang D., Novoselov K.S., Roth S., Geim A.K. Raman Spectrum of Graphene and Graphene Layers. *Phys. Rev. Lett.*, **97,** 187401 (2006).

[3] Yoo J.J., Balakrishnan K., Huang J., Meunier V., Sumpter B. G., Srivastava A., Conway M., Reddy Mohana A.L., Yu. J., Vajtai R., Ajayan P.M. Ultrathin Planar Graphene Supercapacitors. *Nano Lett.*, **11**, 1423–1427 (2011).

[4] Novoselov K.S., Jiang D., Schedin F., Booth T.J., Khotkevich V.V., Morozov S.V., Geim A.K. Two-dimensional atomic crystals. *PNAS*, **102**,10451–10453 (2005).

[5] Dössel L., Gherghel L., Feng X., Müllen K. Graphene Nanoribbons by Chemists: Nanometer-Sized, Soluble, and Defect-Free. *Angew. Chem. Int. Ed.*, **50**, 2540–2543 (2011).

[6] Bourlinos A. B., Georgakilas V., Zboril R., Steriotis Th. A., Stubos A. K. Liquid-Phase Exfoliation of Graphite Towards Solubilized Graphenes. *Small*, **5**, 1841–1845 (2009).

[7] Zhu Y., Murali Sh., Stoller M. D., Ganesh K. J., Cai W., Ferreira P. J., Pirkle A., Wallace R. M., Cychosz K. A., Thommes M., Su D., Stach E. A., Ruoff R. S. Carbon-based Supercapacitors Produced by Activation of Graphene. *Science*, **332**, 1537-1541 (2011).

[8] Fan X., Peng W., Li Y., Li X., Wang Sh., Zhang G., Zhang F. Deoxygenation of Exfoliated Graphite Oxide under Alkaline Conditions: A Green Route to Graphene Preparation. *Adv. Mater.*, **20**, 4490–4493 (2008).

[9] Wee G., Mak W.F., Phonthammachai N., Kiebele A., Reddy M.V., Chowdari B.V.R., Gruner G., Srinivasan M., Mhaisalkar S.G. Particle Size Effect of Silver Nanoparticles Decorated Single Walled Carbon Nanotube Electrode for Supercapacitors**.** *J. Electrochem. Soc.*, **157**, A179-A184 (2010).

[10] Zhang G., Zheng L., Zhang M., Guo Sh., Liu Z.-H., Yang Z., Wang Z. Preparation of Ag-Nanoparticle-Loaded MnO2 Nanosheets and Their Capacitance Behavior. *Energy Fuels*, **26**, 618–623 (2012).

[11] Stergiou D.V., Diamanti E.K., Gournis D., Prodromidis M.I. Comparative study of different types of graphenes as electrocatalysts for ascorbic acid. *Electrochem. Commun.*, **12**, 1307–1309 (2010).

[12] Lai L., Chen L., Zhan D., Sun L., Liu J., Lim S. H., Poh Ch.K., Shen Z., Lin J. One-step synthesis of NH_2-graphene from in situ graphene-oxide reduction and its improved electrochemical properties. *Carbon*, **49,** 3250-3257 (2011).

[13] Li W., Tang X-Z., Zhang H.-B., Jiang Z.-G., Yu Z.-Z., Du X.-Sh., Mai Y.-W. Simultaneous surface functionalization and reduction of graphene oxide with octadecylamine for electrically conductive polystyrene composites. *Carbon*, **49**, 4724-4730 (2011).

[14] Feng X.-M., Li R.-M., Ma Y.-W., Chen R.-F., Shi N.-E., Fan Q.-L., Huang W. One-Step Electrochemical Synthesis of Graphene/Polyaniline Composite Film and Its Applications. *Adv. Funct. Mater.*, **21**, 2989–2996 (2011).

[15] Park S., An J., Potts J.R., Velamakanni A., Murali S., Ruoff R Hydrazine-reduction of graphite- and graphene oxide. *Carbon*, **49**, 3019-3023 (2011).

[16] Teng Ch.-Ch., Ma Ch.-Ch. M., Lu Ch.-H., Yang Sh.-Y., Lee Sh. H., Hsiao M.-Ch., Yen M.-Y., Chiou K.-Ch., Lee T.-M. Thermal conductivity and structure of non-covalent functionalized graphene/epoxy composites. *Carbon*, **49**, 5107 –5116 (2011).

[17] Graf D., Molitor F., Ensslin K., Stampfer C., Jungen A., Hierold C., Wirtz L. Spatially Resolved Raman Spectroscopy of Single and Few-Layer Graphene. *Nano Lett*, *7*, 238-242 (2007).

[18] Fan Z.-J., Kai W., Yan J., Wei T., Zhi L.-J., Feng J., Ren Y.-M., Song L.-P., Wei F. Facile Synthesis of Graphene Nanosheets *via* Fe Reduction of Exfoliated Graphite Oxide. *ACS Nano*, **5**, 191–198 (2011).

[19] Hao Y., Wang Y., Wang L., Ni Z., Wang Z., Wang R., Koo Ch.K., Shen Z., Thong J.T. L. Probing Layer Number and Stacking Order of Few-Layer Graphene by Raman Spectroscopy. *Small*, **6**, 195–200 (2010).

[20] Rout Ch.S., Kumar A., Fisher T.S. Carbon nanowalls amplify the surface-enhanced Raman scattering from Ag nanoparticles. *Nanotechnology*, **22**, 395704 (2011).